Article

Investigation of the Effect of Physical Ability on the Fall Mitigation Motion Using the Combination of Experiment and Simulation

Yasuhiro Akiyama [1,*] , Shuto Yamada [2], Shogo Okamoto [3] and Yoji Yamada [4]

1 Faculty of Textile Science and Technology, Shinshu University, Nagano 386-8567, Japan
2 Department of Mechanical Systems Engineering, Nagoya University, Aichi 464-8601, Japan
3 Department of Computer Science, Tokyo Metropolitan University, Tokyo 191-0065, Japan
4 National Institute of Technology, Toyota College, Aichi 471-0067, Japan
* Correspondence: akiyama_yasuhiro@shinshu-u.ac.jp

Abstract: The simulation of fall plays a critical role in estimating injuries caused by fall. However, implementing human fall mitigation motions on a simulator proves challenging due to the complexity and variability of fall movement. Our simulator estimates fall motion by extrapolating the motion observed in fall experiments. By incorporating actual fall motion data for the upper limbs, we enhanced the realism of the fall simulation. The application of forward dynamics control to the lower limbs allowed for the adjustment of mitigation motions, taking into account individual physical capabilities. In this study, fall simulations were conducted under the constraints of maximum joint torque and maximum torque change rate, emulating the physical capabilities of both the elderly and young adults. Our results successfully demonstrated the mitigation motion facilitated by the stance leg reduced the descent velocity of the center of mass by 0.75 m/s for elderly individuals and by 1.25 m/s for young adults, compared to a zero torque condition. This indicates that our study introduced a novel method for quantifying the impact of the lower limbs' physical capabilities on fall velocity. Such a method represents a significant advancement in understanding how mitigation motions can influence fall injury simulations.

Keywords: fall simulation; mitigation motion; physical capability

1. Introduction

Falls constitute a significant societal issue in aging societies. Falls occurring in everyday life and industrial settings often lead to bone fractures or fatalities, inflicting substantial societal losses [1]. Predominant causes of falling include tripping and slipping. Robinovitch et al. [2] reported that the most common causes of fall among the elderly are incomplete weight transfer and tripping. Falls account for 24% of work-related injuries necessitating at least four days of rest.

Research related to fall movements is divided into two main categories: experimental and simulated studies. While fall experiments facilitate the observation and measurement of actual human movements, ethical and safety concerns impose limitations on experimental conditions. In most cases, safety measures such as using mats [3,4] or support harnesses [5] constrain the scenarios and motion variations from actual fall. Although simulations provide a higher degree of flexibility in creating fall scenarios, they cannot replicate active human reactions, such as defensive or mitigation actions against fall [6].

An experimental study explored the factors influencing successful fall avoidance motions in the elderly (i.e., quick and extended recovery steps after tripping) [7]. In an experiment aimed at estimating impact force during a fall, researchers reported an approximate load of 350 N exerted on the wrist in a scenario where a fall occurred from a standing position onto a protective mattress [8]. In another study, the changes in ground

reaction force due to variations in hand placement were measured when falling from midway in a falling posture [9,10]. Furthermore, it was also observed that the speed and force of the mitigation motion that uses arms were affected by aging [11], which suggests that the effectiveness of mitigation motion differs among individuals. Additionally, we conducted a tripping experiment under conditions that restricted the recovery step, making the fall inevitable, to evaluate the relationship between the length of the recovery step and the descent velocity of the center of mass (CoM) [12].

In simulations, humans were modeled as rigid body links connected with rotational joints. Multibody simulations can estimate the impact of a fall by sequentially simulating the progression of fall movements [13]. These simulations can estimate ground reaction force under various fall conditions. However, some simulation conditions, such as locking or zero-torque of joint angles, differ from the actual human fall conditions [6,14]. A study estimated changes in falling speed and time duration by accounting for differences in walking speed as initial conditions [15]. Nevertheless, some simulators estimate movements exclusively in the sagittal plane, which is more suitable for simulating symmetric motion. Moreover, simulation studies commonly encounter the issue that base fall movements are either artificial or not based on the actual fall motion. Therefore, the validity of simulated fall behaviors is uncertain.

Fall avoidance has been also researched in the field of robotics. Especially the control strategy of biped robots is useful for the stability analysis of human gait [16]. However, it is not reasonable to apply the control strategy of the humanoid robot to actual humans because the motion strategy of humans is not identified sufficiently. The reaction strategy of humans was investigated in experiments [3,17]. Considering the uncertainty and variation of human motion, simple reaction patterns such as arm stretch and leg brace are more applicable for human fall simulation.

To accurately assess the impact of varying fall mitigation strategies on resultant injuries, it is essential to model fall movements based on specific mitigation techniques such as arming and bracing. Furthermore, the realism of motion estimation improves as the duration of the motion simulation is reduced due to a decrease in the variability introduced by the uncertainty of the simulation algorithm. Therefore, it is advantageous to focus the extrapolation primarily on the terminal phase of the fall movement. Under these conditions, variations in human physical capabilities serve as a critical parameter for mitigation motion, potentially leading to distinct fall dynamics. It is hypothesized that limiting joint torque, particularly in supporting the stance leg, may reduce the ability to decelerate the body's descent speed effectively.

In this study, we estimated fall movements by integrating experimental observations and three-dimensional simulations, focusing primarily on forward fall resulting from tripping. We aimed to enhance the realism of fall behavior by extrapolating measured movements from experiments predicting an actual fall. Additionally, simulations under various conditions, representing a decrease in joint torques due to aging, were performed to evaluate the impact of physical capabilities on falling hazards. The simulator developed in this study facilitates the estimation of fall hazard severity by integrating human mitigation actions and reproducing natural falling movements.

2. Methods

2.1. Fall Movement

2.1.1. Overview

The fall movements obtained from experiments reported in reference [12] served as the basis for the simulation in this study. We conducted experiments wherein falls described in detail below were artificially induced by causing participants to trip and stumble while walking [12]. Movements were measured using an optical motion capture system (MAC3D System, Motion Analysis Corp., Rohnert Park, CA, USA). As participants were secured by a protective harness before making contact with the ground, only the movements until the point of support can be considered genuine fall movements. Because the harness was

supported by an air spring, the participant was gradually unloaded as the body descended. In all trials, the hands contacted the ground after weight support, indicating that a fall would have occurred in the absence of the harness.

Figure 1a illustrates the configuration of the tripping apparatus utilized in this study. Subjects traversed a 7 m walking lane and encountered randomized tripping incidents. An obstacle, positioned to strike the subject's toe at a height of 25 cm, was secured on the ground to initiate a trip. To induce a fall, the recovery leg's ankle was tethered with a rope, and the recovery step length was deliberately restricted. Adjustments to the obstacle's position and the rope's length were made to ensure that tripping occurred at precise, controlled timing.
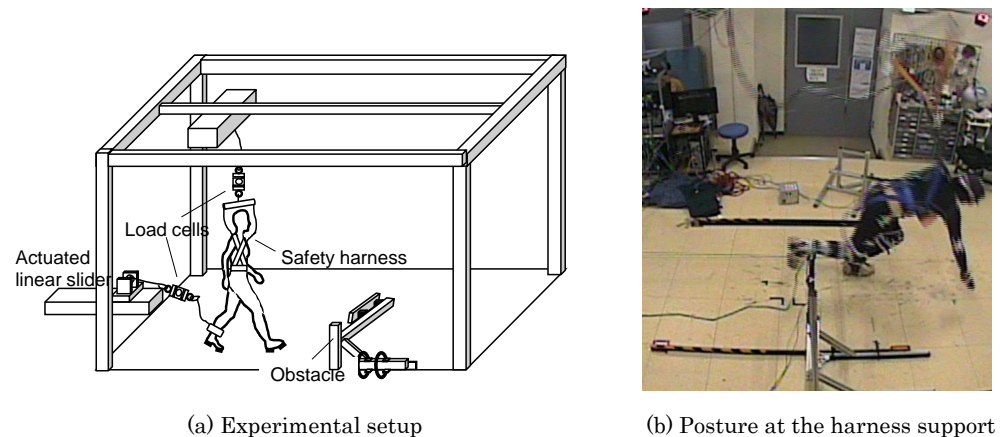

(a) Experimental setup

(b) Posture at the harness support

Figure 1. Overview of fall experiment.

During the experiments, tripping was induced in the late swing phase of the gait cycle, and a "lowering strategy", in which people stepped the tripped leg on site instantaneously and subsequently stepped the other leg forward, was observed, as previously reported [18]. Upon tripping, subjects immediately lowered the affected leg and braced for impact, followed by the forward motion of the opposite leg in an attempt to stabilize and support the body's forward momentum. However, due to the restricted length of the recovery step, control over the forward momentum was not achievable, leading to an inevitable forward fall, as depicted in Figure 1b. This figure shows the left leg attempting a forward step after the right leg is tripped.

2.1.2. Participant

The experiments were conducted on seven young adults (mean and standard deviation of age 21.4 ± 1.2 years, height 172.91 ± 3.24 cm, weight 61.03 ± 7.59 kg). All participants were free of any symptoms or medications that could influence body motion, balance, or reaction time. Additionally, they were not experiencing any physiological discomforts that could impact their performance during the study.

2.1.3. Data Overview

A total of 58 falls under two conditions, the maximum limitation of the recovery step length of 0 cm (not stepping over the obstacle) and 20 cm, were observed. Further details are described in a published paper [12]. Fall simulation was performed to extrapolate the posture and velocity obtained at the timing of harness support when the natural fall motion ended. The representative posture at the timing of harness support is shown in Figure 1b.

2.2. Fall Simulation

2.2.1. Model and Physical Limits

The fall simulator was constructed using MATLAB's Simulink toolbox and Simscape Multibody (MathWorks, Inc., Natick, MA, USA). The human model consisted of 14 rigid

body links, including the and right limbs for the foot, lower leg, thigh, hand, forearm, and upper arm, as well as pelvis and trunk. Head and neck were incorporated into the trunk link. The model's size, mass, and inertia were scaled based on the participants' height and weight [19,20]. The parameter of the simulation model is shown in Table 1. This model comprised 11 joints, including left and right ankles, knee, hip, shoulder, and elbow joints, and lumbar spine. The hip, shoulder, and lumbar joints have three degrees of freedom (DOFs), while the remaining joints have one DOF. The foot link of the supporting leg and the floor surface were connected via a virtual six-DOF joint.

Table 1. Parameters of the simulation model (M: body mass, H: height) [19,20].

Segment	Mass	Length	Mass Center Position [%]	Inertia [kg·cm^2]
Head and Neck	0.069 M	0.140 H	59.8 (from top)	1.43 M + 1.73 H − 112 1.17 M + 1.52 H − 78 1.72 M + 0.08 H + 61.6
Trunk	0.160 M	0.139 H	50.7 (from neck)	18.30 M − 5.73 H + 367 36.03 M − 9.98 H + 561 36.73 M − 5.97 H + 81.2
Abdomen	0.163 M	0.124 H	45.0 (from trunk)	26.70 M − 8.00 H + 263 43.14 M − 19.80 H + 1501 39.80 M − 12.87 H + 618.5
Pelvis	0.112 M	0.084 H	61.1 (from abdomen)	11.80 M + 3.44 H − 934 14.70 M + 1.69 H − 775 12.00 M + 7.74 H − 1568
Upper arm	0.027 M	0.162 H	57.7 (from shoulder)	1.53 M + 1.34 H − 232 1.56 M + 1.51 H − 250.7 0.55 M + 0.04 H − 16.9
Forearm	0.016 M	0.154 H	45.7 (from elbow)	0.86 M + 0.38 H − 67.9 0.95 M + 0.34 H − 64 0.31 M + 0.09 H + 5.66
Hand	0.006 M	0.050 H	79.0 (from wrist)	0.08 M + 0.03 H − 6.26 0.09 M + 0.09 H − 13.68 0.17 M + 0.12 H − 19.5
Thigh	0.142 M	0.243 H	41.0 (from hip)	32.02 M + 19.24 H − 3690 31.70 M + 18.61 H − 3557 11.30 M − 2.28 H − 13.5
Shank	0.043 M	0.249 H	44.6 (from knee)	4.59 M + 6.82 H − 1152 4.59 M + 6.63 H − 1105 1.13 M + 0.30 H − 70.5
Foot	0.013 M	0.148 H	44.2 (from heel)	0.41 M + 0.61 H − 97.09 0.14 M + 0.09 H − 15.48 0.48 M + 0.63 H − 100

The moments of inertia are presented in the following order: mediolateral axis, anterior–posterior axis, and vertical axis. The units for mass (M) and height (H) in the context of inertia are kilograms (kg) and centimeters (cm), respectively.

To consider human physical limitations, constraints were imposed on joint torque and the rate of joint torque change. The torque and torque change rate were determined based on values from the literature [21–27]. The torque and rate of torque change for each condition are shown in Table 2.

Table 2. Maximum torque, maximum torque change rate, and gains of each joint.

	Gain		Max Torque [Nm]		Max Torque Change Rate [Nm/10 ms]	
	Kp/Kd	Direction	Young (20 s)	Elderly (70 s)	Young (20 s)	Elderly (70 s)
Ankle	200/1.5	Dorsal flexion	45	35	3.0	2.0
		Planter flexion	150	100	10	7.0
Knee	200/1.5	Flexion	0	0	13	8.0
		Extension	260	180	13	8.0
Hip	100/1.5	Flexion	0	0	7.5	4.5
		Extension	150	100	7.5	4.5
Lumbar	150/1.5	Backward	0	0	15	8.9
		Forward	300	200	15	8.9

2.2.2. Joint Motion Simulation

First, joint torques of the entire experimental movement, including the harness-supported phase, were calculated through inverse dynamics computations. Given that the supporting harness was omitted in the simulation, the inverse dynamic simulation overestimated the joint torques. Therefore, a forward dynamics analysis with an upper limit on the exerted torque was then performed. The torque acting on each joint was formulated as in Equation (1).

$$\tau = K_p(\theta^{ref} - \theta) + K_d(\dot{\theta}^{ref} - \dot{\theta}) + b(\theta, \dot{\theta}) \tag{1}$$

This is the sum of control torque calculated using Proportional–Differential controller and gravity and inertia torque. The first and second terms were calculated based on the reference joint pattern, which was the joint movement obtained in the experiment. The third term, which consists of gravity and inertial torque, was calculated using the multibody theorem. The fixed-step, stiff solver (ode14x) with a step time of 0.01 s was used for kinematic calculations.

The determination of the proportional (K_p) and derivative (K_d) gains was executed through a methodical trial and error approach. Specifically, we performed a forward dynamics analysis on every experimental trial conducted, without setting any limits on joint torques. This comprehensive analysis aimed to identify gain values and their combinations that consistently resulted in high reproducibility across trials. Gains K_p and K_d are presented in Table 2. Owing to the torque limit that reflected the physical limit of humans, the joint pattern could not be completely reproduced under the physical conditions of the elderly and young.

Due to insufficient understanding of the fall mitigation mechanism, it is challenging to establish an algorithmic posture control policy. Thus, in this study, we focused on the ankle, knee, and hip joints of the supporting leg and lumbar joint, which substantially influence the descent velocity of the body. The forward dynamics method was applied to these joints. In contrast, the joint patterns observed in the experiments were directly applied to the other joints. During the fall movements, participants spread their arms to the sides and moved them forward and downward to support their bodies. This motion appears reasonable even if the harness support does not exist. Thus, the effect of harness support on the upper limbs was ignored in this study.

2.2.3. Process of Fall Simulation

The extrapolation simulation started from the time frame just before harness support, which was the initial condition, and estimated the terminal phase of fall under various mitigation abilities. In the initial posture, the subject was supported on a single leg. The simulation continued as the participant fell forward until either hand or knee made contact with the floor. Three conditions were tested in simulations: a free fall with zero joint torque, a condition with limited joint torque and torque change rate for young adults, and a similar

condition for the elderly. The three conditions of simulation were applied to all trials obtained in the experiments, respectively.

2.3. Data and Statistical Analysis

The body part of the participant that made first contact with the floor was recorded for each trial. The hand or knee of the supporting or swinging leg was the first to contact the ground. The initial CoM heights and descent velocities were compared between long- and short-step conditions using *t*-test. To simply evaluate the impact load upon fall, the contact velocity that was defined as the vertical component of the velocity vector of contact part at the moment of collision was used. The contact velocities, CoM height, and its descent velocity at the timing of collision were compared among three conditions (free fall, young adults, and elderly) using the Wilcoxon signed-rank test with the Bonferroni method. Therefore, the significance levels were established at $p = 0.0017$ for a 5% significance threshold and $p = 0.0033$ for a 1% threshold. Statistical analysis was conducted using the Statistics and Machine Learning Toolbox in MATLAB 2022a. Correlation analyses were performed to assess the relationship between time duration and contact velocity under each experimental condition.

Extrapolation simulations were conducted for 58 trials. Nine trials exhibited unnatural falling behavior and were excluded from the results. Thus, 49 trials were used for further analysis.

3. Results

The initial CoM height and descent velocity are shown in Table 3. Since the harness support starts at a specified height, the variation in the initial CoM height is small. The variation in the contact parts is shown in Table 4. In most trials, the hands made contact with the ground first, but in some trials, the knees made contact with the ground before the hands. There were 12 trials where the contact part changed when joint torque conditions were altered. Among the 12 trials, there were 8 cases where the left and right hands changed, and 2 cases each where the contact part changed from hand to knee or knee to hand. Typical falling movements and joint patterns are shown in Figures 2 and 3. In the experiment, although the subject could not entirely prevent the fall, the harness support allowed for the fall to occur gradually. This means that while the body imbalance could not be corrected, the speed of impact was sufficiently reduced. This motion was identified as the reference motion for successfully mitigating the impact of the fall in this study. However, this motion could not be completely replicated, as the harness support's effects could not be mimicked by altering the torques in the lower limbs. Compared to recorded motions, the simulation model falls faster because of the lack of harness support. Furthermore, in the experiment, the descent speed of the trunk decreased before ground contact, and the ground was reached with both hands and feet almost at the same time. The joint torque of the elderly and young conditions increased to follow the original motion, which was the reference motion of this simulation, under the limitation of torque and torque change rate.

The collision time, which is the time duration of the fall simulation, is shown in Figure 4. Although the time to collision is short due to the simulation beginning at the terminal phase of the fall, the delay in collision due to the generated torque of the lower limbs is apparent. There is a significant difference in collision time between different physical conditions. The collision time for the elderly was shortened by an average of 0.013 s compared to free fall ($p = 3.10 \times 10^{-3}$), while the collision time for young adults was shortened by an average of 0.027 s compared to free fall ($p = 5.28 \times 10^{-6}$).

The contact velocity, which is the descent velocity of the contact point at the time of collision, is shown in Figure 5. There is a significant difference in contact velocity between different physical conditions. In the elderly condition, the contact velocity decreased by an average of 0.73 m/s compared to free fall ($p = 6.26 \times 10^{-10}$), while in the young adult condition, the contact velocity decreased by an average of 1.21 m/s compared to free fall ($p = 1.31 \times 10^{-12}$).
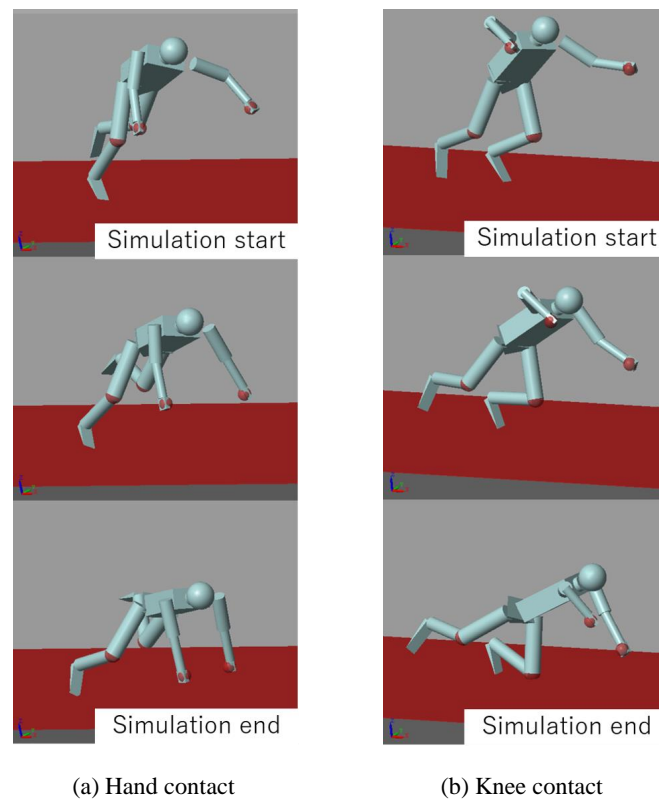
(a) Hand contact　　　　　(b) Knee contact
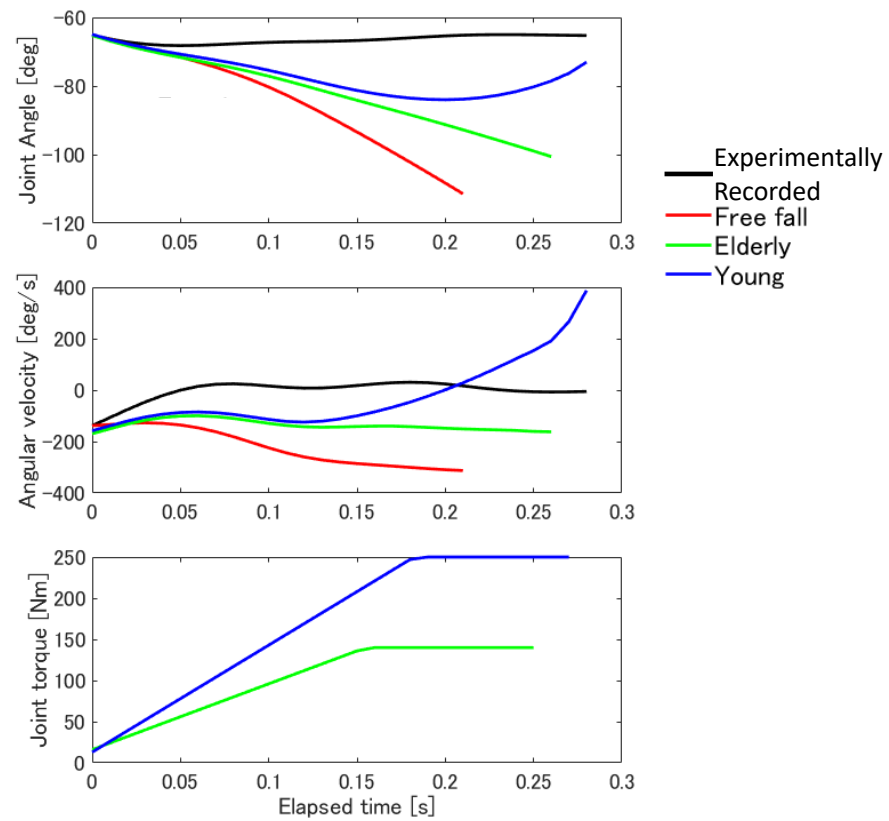
Figure 2. Typical fall movements.

Figure 3. Typical knee joint angle, angle velocity, and joint torque patterns of simulated fall movements.

Table 3. CoM height and CoM descent velocity at initial condition.

	Long-Step Case	Short-Step Case	*p*-Value
Initial height [m]	0.75 ± 0.039	0.76 ± 0.034	0.296
Initial descent velocity [m/s]	-1.0 ± 0.23	-1.1 ± 0.33	0.196

Table 4. Distribution of contact parts.

Contact Part		Free Fall	Elderly	Young
Hand	Support side	16	15	16
	Swing side	24	26	24
Knee	Support side	8	7	8
	Swing side	1	1	1
Total		49	49	49
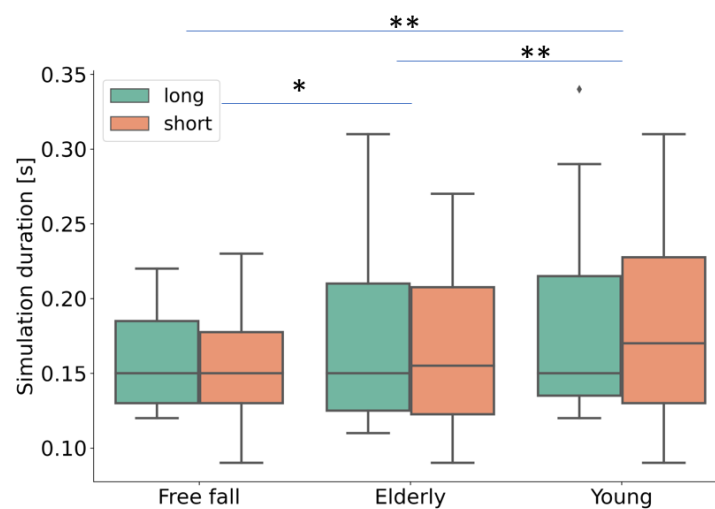
Figure 4. Time duration of fall simulation (◆ means the outlier. *: $p < 0.017$, **: $p < 0.0033$. They are at 5% and 1% significance levels).
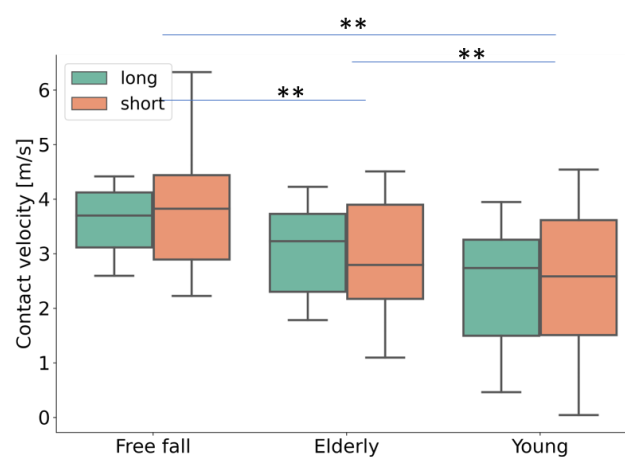
Figure 5. Descent velocity of contact point at the moment of ground contact (**: $p < 0.0033$. They are at 5% and 1% significance levels).

The CoM height and descent velocity at the time of collision are shown in Figures 6 and 7, respectively. There is a significant difference in both CoM height and descent velocity at the time of collision between different physical conditions. In the elderly condition, the CoM height at the time of collision was 0.03 m higher on average compared to free fall

($p = 1.09 \times 10^{-6}$), while in the young adult condition, it was 0.06 m higher on average compared to free fall ($p = 1.60 \times 10^{-9}$). In the elderly condition, the CoM descent velocity at the time of collision was 0.75 m/s lower on average compared to free fall ($p = 1.09 \times 10^{-6}$), while in the young condition, it was 1.25 m/s lower on average compared to free fall ($p = 7.11 \times 10^{-15}$).
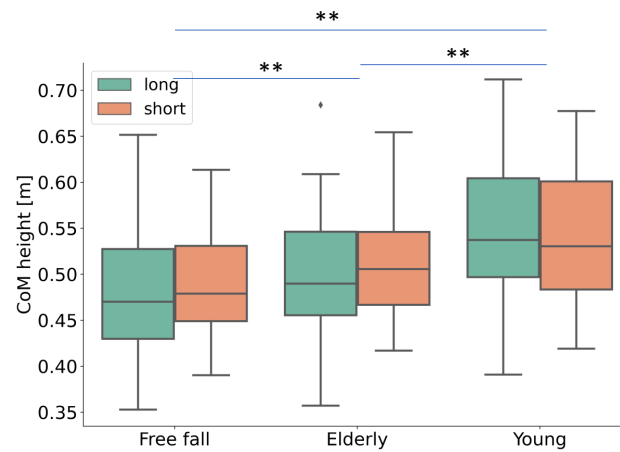

Figure 6. CoM height at the timing of collision (♦ means the outlier. , **: $p < 0.0033$. They are at 5% and 1% significance levels).
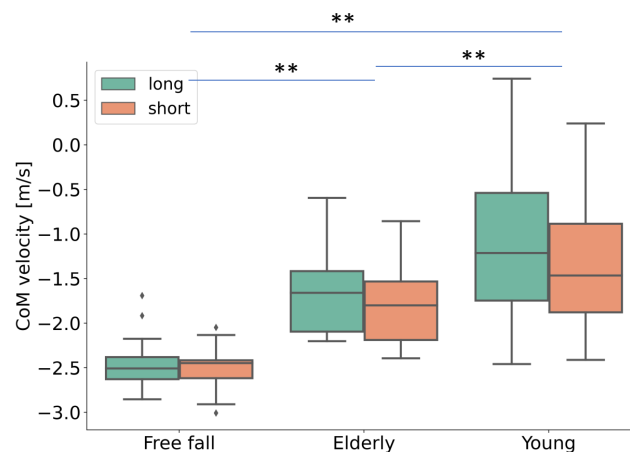
Figure 7. CoM descent velocity at the timing of collision (♦ means the outlier., **: $p < 0.0033$. They are at 5% and 1% significance levels).

4. Discussions

The simulation of falls is critical for analyzing hazardous situations that cannot be directly tested through experiments. However, the diverse range of physical capability and human responses to falling cause uncertainty of motion. This study was designed to elucidate the variance in mitigation motions in response to falls through motion simulation and to quantify the impact of these motions on the severity of fall-related hazards. We evaluated the differences in the joint torque which served as proxies for the physical capabilities of young adults versus the elderly. Our findings successfully demonstrated a reduction in the descent speed of the body attributable to superior physical capabilities.

4.1. The Parameter that Affects Contact Velocity

The scatter plot of contact velocity and collision time is shown in Figure 8. Each condition presents a negative correlation between collision time and contact velocity. This pattern can be attributed to the effect of the bracing of the supporting leg, which mitigates the collision impact. The prolonged collision time corresponds with a larger deceleration of

the contact part. Delaying the time to collision is crucial as it can significantly reduce the speed of impact [3]. Compared to the free condition, distributions for the elderly and young conditions show wider spreads, signifying that the mitigation motion effectively extends the collision time in both these conditions. However, due to the varying distribution of initial posture and velocity, the correlation coefficients are not particularly high.

Contact velocity serves as a primary indicator of impact force, which, in turn, reflects the severity of the fall, as discussed in the literature [28,29]. It was the highest in the free condition, followed by the elderly and young physical conditions, respectively, as shown in Figure 5. Considering the variation in joint torque constraints across different conditions, the action of bracing with the supporting leg appears to play a role in postponing ground contact. Consistent with findings from various studies [30,31], the physical capabilities of an individual are key in managing motion post tripping. This trend aligns with the difference in collision time between conditions as shown in Figure 4, which can be attributed to the deceleration of the trunk due to joint torque in the supporting leg.
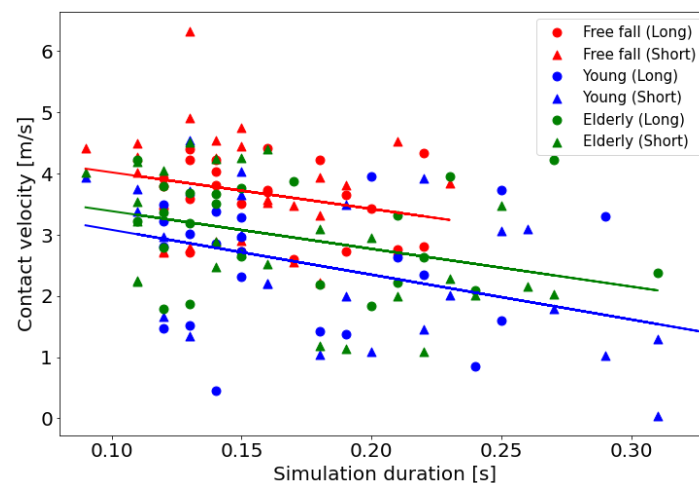

Figure 8. Correlation between time duration and contact velocity ($R = -0.25, -0.36, -0.41$ for free fall, young, and elderly).

On the other hand, a clear correlation exists between contact velocity and CoM descent velocity as shown in Figure 9. Since the movement pattern of upper body joints remains constant across conditions, contact velocity largely functions as CoM descent velocity. The increased impact speed results in a higher impact force [32]. Consequently, these parameters are strongly related to fall-induced injuries. Additionally, collision time influences the movement of contact parts through the motion pattern of upper limb joints. The high correlation coefficient suggests a considerable impact of CoM descent velocity, which is relatively larger than the changes in swing velocity of contact limbs induced by variations in collision timing. While some studies have employed a fixed posture, such as an outstretched hand [32], there have been reports indicating that certain types of arm movements, including elbow flexion [33] and more complex guarding motions [34], can mitigate impact forces. The effect of such a mitigation motion should be considered in future studies.

4.2. The Effect of Condition

The maximum joint torque and the maximum joint torque change rate were ordered from highest to lowest in the free, elderly, and young conditions, respectively. Furthermore, the collision time, contact velocity, CoM height, and CoM descent velocity at the time of collision showed the same pattern. Although CoM height and descent velocity at the time of collision do not directly reflect the collision impact, they can be considered as important indicators of falling behavior. The decrease in CoM descent velocity suggests a deceleration

not only in the descent velocity of the hand and knee contact points but also in the trunk. Such deceleration of the trunk can potentially mitigate the risk and severity of femoral neck fractures and facial contusions, which are crucial factors affecting quality of life [35,36].
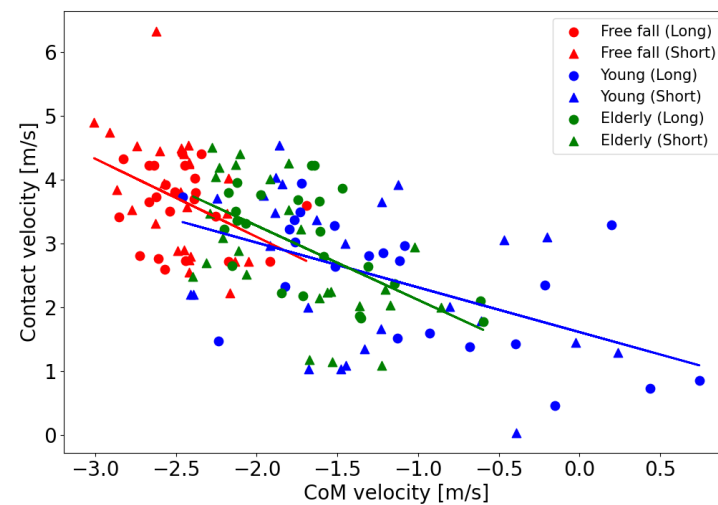

Figure 9. Correlation between contact velocity and CoM descent velocity ($R = -0.39, -0.56, -0.50$ for free fall, young, and elderly).

Successful fall recovery motion is often characterized by an extended recovery step length, a factor attributed to the effective reduction in forward momentum by the bracing force, as noted in previous studies [5,7]. Despite these observations, no significant differences were found between the short-step and long-step conditions across all parameters or conditions. While recovery step length is acknowledged as a factor in successful recovery from tripping, as indicated by the data in Table 3, there were no significant variations in initial CoM height and speed between long-step and short-step conditions. Nevertheless, it is important to recognize that the absence of significant differences in these specific metrics does not negate the potential relationship between recovery step length and the severity of fall injuries.

4.3. Limitations

Although we used the descent velocity of the contact point as an index of collision load, it represents just one factor influencing the interaction force. To estimate the collision load more accurately, the effective mass, which was calculated based on body posture, and the viscoelasticity of human tissue should be considered [13,37].

Additionally, we derived target joint angles and angular velocities directly from the movements observed in our experiment. However, in real situations, humans might employ more complex strategies to avoid fall. For instance, a study by Lauren J. Lattimer et al. suggested that increasing the elbow joint's angular velocity upon ground contact could enhance energy absorption during a fall [11]. Also, employing a trained reaction strategy could be beneficial in mitigating fall injuries [38]. The implementation of such defensive movement algorithms might prove effective in harm reduction.

Typically, aging adversely affects various aspects of gait ability. In this study, we took into consideration only the reduction in muscle strength and muscle activation speed due to aging. However, other factors such as delayed reaction time and decreased balance sensation are likely to influence fall movement. Therefore, it would be beneficial to consider the impact of aging on fall movement more comprehensively.

The diversity of fall motions should also be taken into account, as well as the limitation posed by the small number of participants involved in the study. The experimental dataset encompasses two conditions across seven subjects, which may not be fully representative of the broader population. Employing a range of perturbation patterns is crucial for examining

the general trends in human mitigation strategies. To address the potential impact of the limited sample size, future studies should consider expanding the number of subjects and including a wider variety of fall scenarios. This would enhance the generalizability of the findings and provide a more comprehensive understanding of the different strategies individuals employ to mitigate falls.

5. Conclusions

This study presents simulations of mitigation movements taken during critical fall situations. These simulations are based on movements observed in fall experiments, with a particular focus on forward fall induced by tripping perturbations. Extrapolation simulations performed using these observed movements enabled the estimation of posture and motion leading to ground collisions. As part of the mitigation strategies, supportive torque was applied to the joints of the support leg and lumbar spine, with actuation accomplished using forward dynamics.

Maximum exertion torque and maximum torque change rate for each joint were limited, taking into account the physical capabilities of the elderly and young adults. This methodology facilitated an evaluation of the impact of aging on fall mitigation movements and related hazards. Significant differences in the CoM descent velocity at the timing of collision were discovered among all groups: free fall, elderly, and young. These findings highlight the influence of joint torque in reducing descent velocity. Additionally, numerous other parameters exhibited significant differences across conditions.

The velocity at which ground contact occurs is a crucial parameter for estimating fall injuries as reduced speed at ground contact can mitigate the force of impact. Consequently, this study represents a critical effort to estimate the severity of fall-related hazards by predicting potential mitigation movements in high-risk situations. It is anticipated that the findings can contribute to the development of effective fall mitigation strategies and actions aimed at minimizing fall-related hazards in the future.

References

1. Luukinen, H.; Herala, M.; Koski, K.; Honkanen, R.; Laippala, P.; Kivelä, S.L. Fracture risk associated with a fall according to type of fall among the elderly. *Osteoporos. Int.* **2000**, *11*, 631–634. [CrossRef] [PubMed]
2. Robinovitch, S.N.; Feldman, F.; Yang, Y.; Schonnop, R.; Leung, P.M.; Sarraf, T.; Sims-Gould, J.; Loughin, M. Video capture of the circumstances of falls in elderly people residing in long-term care: An observational study. *Lancet* **2013**, *381*, 47–54. [CrossRef]
3. Feldman, F.; Robinovitch, S.N. Reducing hip fracture risk during sideways falls: Evidence in young adults of the protective effects of impact to the hands and stepping. *J. Biomech.* **2007**, *40*, 2612–2618. [CrossRef] [PubMed]
4. Sabick, M.; Hay, J.; Goel, V.; Banks, S. Active responses decrease impact forces at the hip and shoulder in falls to the side. *J. Biomech.* **1999**, *32*, 993–998. [CrossRef] [PubMed]
5. Pavol, M.J.; Owings, T.M.; Foley, K.T.; Grabiner, M.D. Mechanisms leading to a fall from an induced trip in healthy older adults. *J. Gerontol. Ser. A Biol. Sci. Med Sci.* **2001**, *56*, M428–M437. [CrossRef] [PubMed]

6. Lo, J.; Ashton-Miller, J. Effect of pre-impact movement strategies on the impact forces resulting from a lateral fall. *J. Biomech.* **2008**, *41*, 1969–1977. [CrossRef] [PubMed]

7. Grabiner, M.D.; Koh, T.J.; Lundin, T.M.; Jahnigen, D.W. Kinematics of recovery from a stumble. *J. Gerontol.* **1993**, *48*, M97–M102. [CrossRef]

8. Burkhart, T.A.; Clarke, D.; Andrews, D.M. Reliability of impact forces, hip angles and velocities during simulated forward falls using a novel Propelled Upper Limb fall ARrest Impact System (PULARIS). *J. Biomech. Eng.* **2012**, *134*, 1–8. [CrossRef] [PubMed]

9. Abdolshah, S.; Rajaei, N.; Akiyama, Y.; Yamada, Y.; Okamoto, S. Longitudinal rollover strategy as effective intervention to reduce wrist injuries during forward fall. *IEEE Robot. Autom. Lett.* **2018**, *3*, 4187–4192. [CrossRef]

10. Abdolshah, S.; Rajaei, N.; Akiyama, Y.; Yamada, Y.; Okamoto, S. Investigation into hand impact force during forward falls on uneven terrain. *Int. J. Precis. Eng. Manuf.* **2020**, *21*, 509–517. [CrossRef]

11. Lattimer, L.J.; Lanovaz, J.L.; Farthing, J.P.; Madill, S.; Kim, S.Y.; Robinovitch, S.; Arnold, C.M. Biomechanical and physiological age differences in a simulated forward fall on outstretched hands in women. *Clin. Biomech.* **2018**, *52*, 102–108. [CrossRef] [PubMed]

12. Akiyama, Y.; Mitsuoka, K.; Okamoto, S.; Yamada, Y. Experimental analysis of the fall mitigation motion caused by tripping based on the motion observation until shortly before ground contact. *J. Biomech. Sci. Eng.* **2019**, *14*, 18–00510. [CrossRef]

13. Grzelczyk, D.; Biesiacki, P.; Mrozowski, J.; Awrejcewicz, J. Dynamic simulation of a novel "broomstick" human forward fall model and finite element analysis of the radius under the impact force during fall. *J. Theor. Appl. Mech.* **2018**, *56*, 239–253. [CrossRef]

14. Abdolshah, S.; Akiyama, Y.; Mitsuoka, K.; Yamada, Y.; Okamoto, S. Analysis of upper extremity motion during trip-induced falls. In Proceedings of the 2017 26th IEEE International Symposium on Robot and Human Interactive Communication (RO-MAN), Lisbon, Portugal, 28–31 August 2017; pp. 1485–1490.

15. Klemetti, R.; Moilanen, P.; Avela, J.; Timonen, J. Effects of gait speed on stability of walking revealed by simulated response to tripping perturbation. *Gait Posture* **2014**, *39*, 534–539. [CrossRef]

16. Sugihara, T.; Nakamura, Y.; Inoue, H. Real-time humanoid motion generation through ZMP manipulation based on inverted pendulum control. In Proceedings of the 2002 IEEE International Conference on Robotics and Automation (Cat. No. 02CH37292), Washington, DC, USA, 11–15 May 2002; Volume 2, pp. 1404–1409.

17. Troy, K.L.; Grabiner, M.D. Asymmetrical ground impact of the hands after a trip-induced fall: experimental kinematics and kinetics. *Clin. Biomech.* **2007**, *22*, 1088–1095. [CrossRef] [PubMed]

18. Roos, P.E.; McGuigan, M.P.; Trewartha, G. The role of strategy selection, limb force capacity and limb positioning in successful trip recovery. *Clin. Biomech.* **2010**, *25*, 873–878. [CrossRef] [PubMed]

19. Zatsiorsky, V. The mass and inertia characteristics of the main segments of the human body. *Biomechanics* **1983**, 1152–1159.

20. De Leva, P. Adjustments to Zatsiorsky-Seluyanov's segment inertia parameters. *J. Biomech.* **1996**, *29*, 1223–1230. [CrossRef]

21. Thelen, D.G.; Schultz, A.B.; Alexander, N.B.; Ashton-Miller, J.A. Effects of age on rapid ankle torque development. *J. Gerontol. Ser. A Biol. Sci. Med Sci.* **1996**, *51*, M226–M232. [CrossRef]

22. Sale, D.; Quinlan, J.; Marsh, E.; McComas, A.; Belanger, A. Influence of joint position on ankle plantarflexion in humans. *J. Appl. Physiol.* **1982**, *52*, 1636–1642.

23. Marsh, E.; Sale, D.; McComas, A.; Quinlan, J. Influence of joint position on ankle dorsiflexion in humans. *J. Appl. Physiol.* **1981**, *51*, 160–167. [CrossRef]

24. Simoneau, E.; Martin, A.; Van Hoecke, J. Muscular performances at the ankle joint in young and elderly men. *J. Gerontol. Ser. A Biol. Sci. Med. Sci.* **2005**, *60*, 439–447. [CrossRef]

25. Bento, P.C.B.; Pereira, G.; Ugrinowitsch, C.; Rodacki, A.L.F. Peak torque and rate of torque development in elderly with and without fall history. *Clin. Biomech.* **2010**, *25*, 450–454. [CrossRef]

26. Harbo, T.; Andersen, H.; Jakobsen, J. Length-dependent weakness and electrophysiological signs of secondary axonal loss in chronic inflammatory demyelinating polyradiculoneuropathy. *Muscle Nerve* **2008**, *38*, 1036–1045. [CrossRef] [PubMed]

27. Harbo, T.; Brincks, J.; Andersen, H. Maximal isokinetic and isometric muscle strength of major muscle groups related to age, body mass, height, and sex in 178 healthy subjects. *Eur. J. Appl. Physiol.* **2012**, *112*, 267–275. [CrossRef]

28. Abdolshah, S.; Rajaei, N.; Akiyama, Y.; Yamada, Y.; Okamoto, S. Safety considerations for forward falls. *J. Musculoskelet. Neuronal Interact.* **2020**, *20*, 176. [PubMed]

29. Chiu, J.; Robinovitch, S.N. Prediction of upper extremity impact forces during falls on the outstretched hand. *J. Biomech.* **1998**, *31*, 1169–1176. [CrossRef] [PubMed]

30. Pijnappels, M.; Bobbert, M.F.; van Dieën, J.H. Push-off reactions in recovery after tripping discriminate young subjects, older non-fallers and older fallers. *Gait Posture* **2005**, *21*, 388–394. [CrossRef] [PubMed]

31. Pijnappels, M.; Reeves, N.D.; Maganaris, C.N.; Van Dieen, J.H. Tripping without falling; lower limb strength, a limitation for balance recovery and a target for training in the elderly. *J. Electromyogr. Kinesiol.* **2008**, *18*, 188–196. [CrossRef]

32. Kawalilak, C.; Lanovaz, J.; Johnston, J.; Kontulainen, S. Linearity and sex-specificity of impact force prediction during a fall onto the outstretched hand using a single-damper-model. *J. Musculoskelet. Neuronal Interact.* **2014**, *14*, 286–293.

33. DeGoede, K.; Ashton-Miller, J. Fall arrest strategy affects peak hand impact force in a forward fall. *J. Biomech.* **2002**, *35*, 843–848. [CrossRef]

34. Groen, B.E.; Weerdesteyn, V.; Duysens, J. Martial arts fall techniques decrease the impact forces at the hip during sideways falling. *J. Biomech.* **2007**, *40*, 458–462. [CrossRef] [PubMed]

35. Caplan, B.; Bogner, J.; Brenner, L.; Yang, Y.; Mackey, D.C.; Liu-Ambrose, T.; Leung, P.M.; Feldman, F.; Robinovitch, S.N. Clinical risk factors for head impact during falls in older adults: A prospective cohort study in long-term care. *J. Head Trauma Rehabil.* **2017**, *32*, 168–177.

36. Yang, Y.; Komisar, V.; Shishov, N.; Lo, B.; Korall, A.M.; Feldman, F.; Robinovitch, S.N. The effect of fall biomechanics on risk for hip fracture in older adults: A cohort study of video-captured falls in long-term care. *J. Bone Miner. Res.* **2020**, *35*, 1914–1922. [CrossRef] [PubMed]

37. Robinovitch, S.N.; Hayes, W.C.; McMahon, T.A. Distribution of contact force during impact to the hip. *Ann. Biomed. Eng.* **1997**, *25*, 499–508. [CrossRef]

38. Van der Zijden, A.; Groen, B.; Tanck, E.; Nienhuis, B.; Verdonschot, N.; Weerdesteyn, V. Can martial arts techniques reduce fall severity? An in vivo study of femoral loading configurations in sideways falls. *J. Biomech.* **2012**, *45*, 1650–1655. [CrossRef]